

# Broadly tunable source around 2050 nm based on wideband parametric conversion and thulium–holmium amplification cascade

Adrien Billat,<sup>\*</sup> Steevy Cordette, and Camille-Sophie Brès

Photonic Systems Laboratory, Ecole Polytechnique Fédérale de Lausanne (EPFL) STI IEL, CH-1015, Lausanne, Switzerland

<sup>\*</sup>[adrien.billat@epfl.ch](mailto:adrien.billat@epfl.ch)

**Abstract:** We report the design of a short-wave infrared continuous-wave light source featuring a 20 mW average output power, and with a wavelength that can be freely selected in the 2000–2100 nm range amid a low power ripple. The operating principle relies on the simultaneous broadband parametric conversion of two seeds in a highly nonlinear silica fiber pumped in the L-band followed by amplification and equalization in an appended thulium- and holmium-doped fiber cascade directly pumped by their respective previous stage.

©2014 Optical Society of America

**OCIS codes:** (190.4975) Parametric processes; (230.2285) Fiber devices and optical amplifiers; (060.4370) Nonlinear optics, fibers; (140.3070) Infrared and far-infrared lasers.

---

## References and links

1. S. Moro, A. Danicic, N. Alic, N. G. Usechak, and S. Radic, "Widely-tunable parametric short-wave infrared transmitter for CO<sub>2</sub> trace detection," *Opt. Express* **19**(9), 8173–8178 (2011).
  2. M. N. Petrovich, F. Poletti, J. P. Wooller, A. M. Heidt, N. K. Baddela, Z. Li, D. R. Gray, R. Slavík, F. Parmigiani, N. V. Wheeler, J. R. Hayes, E. Numkam, L. Gruner-Nielsen, B. Pálsdóttir, R. Phelan, B. Kelly, J. O'Carroll, M. Becker, N. MacSuibhne, J. Zhao, F. C. Gunning, A. D. Ellis, P. Petropoulos, S. U. Alam, and D. J. Richardson, "Demonstration of amplified data transmission at 2 μm in a low-loss wide bandwidth hollow core photonic bandgap fiber," *Opt. Express* **21**(23), 28559–28569 (2013).
  3. Z. Li, S. U. Alam, Y. Jung, A. M. Heidt, and D. J. Richardson, "All-fiber, ultra-wideband tunable laser at 2 μm," *Opt. Lett.* **38**(22), 4739–4742 (2013).
  4. J. Li, Z. Sun, H. Luo, Z. Yan, K. Zhou, Y. Liu, and L. Zhang, "Wide wavelength selectable all-fiber thulium doped fiber laser between 1925 nm and 2200 nm," *Opt. Express* **22**(5), 5387–5399 (2014).
  5. N. Simakov, A. Hemming, W. A. Clarkson, J. Haub, and A. Carter, "A cladding-pumped, tunable holmium doped fiber laser," *Opt. Express* **21**(23), 28415–28422 (2013).
  6. <http://www.eospace.com>
  7. F. Gholami, B. P.-P. Kuo, S. Zlatanovic, N. Alic, and S. Radic, "Phase-preserving parametric wavelength conversion to SWIR band in highly nonlinear dispersion stabilized fiber," *Opt. Express* **21**(9), 11415–11424 (2013).
  8. A. Billat, S. Cordette, Y. P. Tseng, S. Kharitonov, and C.-S. Brès, "High-power parametric conversion from near-infrared to short-wave infrared," *Opt. Express* **22**(12), 14341–14347 (2014).
  9. M. E. Marhic, K. K.-Y. Wong, and L. G. Kazovsky, "Wide-band tuning of the gain spectra of one-pump fiber optical parametric amplifiers," *IEEE J. Sel. Top. Quantum Electron.* **10**(5), 1133–1141 (2004).
  10. S. D. Agger and J. H. Povlsen, "Emission and absorption cross section of thulium doped silica fibers," *Opt. Express* **14**(1), 50–57 (2006).
  11. F. Gholami, S. Zlatanovic, E. Myslivets, S. Moro, B. P.-P. Kuo, C.-S. Brès, A. O. J. Wiberg, N. Alic, and S. Radic, "10Gbps Parametric Short-Wave Infrared Transmitter," in *Optical Fiber Communication Conference, OSA Technical Digest (CD)* (Optical Society of America, 2011), paper OThC6.
  12. S. Cordette, A. Billat, Y.-P. Tseng, and C.-S. Brès, "Tunable Thulium-Assisted Parametric Generation of 10 Gb/s Intensity Modulated Signals Near 2 μm," in *Optical Communication (ECOC 2014), 40th European Conference and Exhibition on (Cannes, 2014)*, paper P.1.12.
- 

## 1. Introduction

The short-wave infrared (SWIR) sub-interval comprising wavelengths from 2000 nm to 2100 nm has recently gathered a significant interest for LIDAR-based CO<sub>2</sub> sensing [1] and could

potentially become part of a new telecommunication window in the near future [2]. Narrow linewidth, modulation capable and broadly tunable laser sources are of primary interest for these two applications. Recent development in fiber lasers have shown the emergence of medium power ( $\sim 10$  mW) tunable continuous-wave (CW) thulium-doped fiber lasers [3] as well as much more powerful ones (several watts) but with complex wavelength tuning mechanism [4]. Closely related, a demonstration of a tunable high power laser emitting around  $2.1 \mu\text{m}$  and based on a cladding-pumped holmium-doped fiber (HDF) can be found in [5]. The output of medium power lasers around 2000 nm can eventually be modulated in phase or intensity with an expensive fiber-optics modulator designed especially for this band [6] and operating to several GHz. However it is more complex to apply the same fast processing to high power (more than a few Watts), free space laser beams. Moreover the filtering elements in the aforementioned powerful laser cavities are either Bragg gratings or diffraction gratings, which in the one case does not allow broad tuning range and in the other does not guarantee accurate wavelength stability with respect to mechanical perturbations. A viable alternative approach to obtain tunable SWIR sources is to use degenerate four-wave mixing (FWM) in highly nonlinear fibers (HNLF) [7]. However the low conversion efficiency obtained over such broadband operation limits the wavelength tunability. Wavelength selection is possible but generally requires spectral tuning of both the signal and the high-power pump, which is not always practical.

In this letter we present an improvement of our all-silica-fiber source, based on the cavity-less association of a fiber optical parametric amplifier (FOPA) and a thulium-doped fiber amplifier (TDFA), which has shown to output up to 700 mW of CW power around 1950 nm [8]. This source is modified in order to reach wavelengths up to  $2.1 \mu\text{m}$  with the addition of a HDF amplification stage, of which the pump is generated in a power efficient way from the FOPA-TDFA assembly. We also demonstrate that mode-hop free wavelength selection is possible over more than 60 nm, maintaining a power level between 10 and 15 dBm and an optical signal-to-noise ratio (OSNR) higher than 25 dB.

## 2. Operating principle and experimental setup

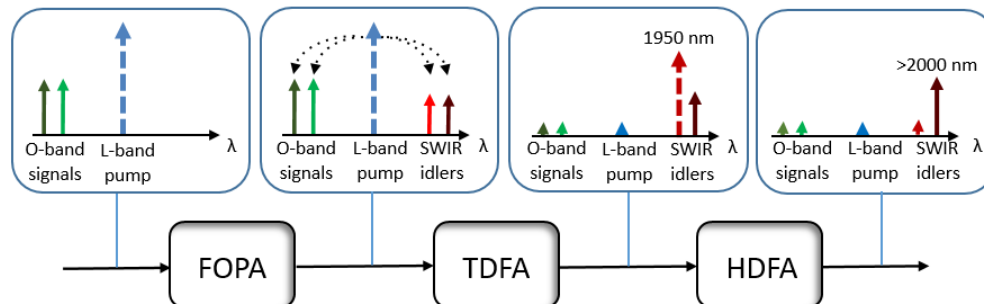


Fig. 1. Schematic of the idlers generation and amplification in each stage. The dashed arrows correspond to the pumps for each stage: blue arrow is the pump for both the parametric process and the TDFA, red arrow is the pump for the HDFA.

The source relies partly on a previously demonstrated design based on FWM in a HNLF to generate light around 1950 nm from conventional telecommunication lasers and electro-optical devices. The frequency mixing in the HNLF occurs between a signal wave located in the O-band (1250-1360 nm) and a high power CW pump located in the L-band to create an idler wave in the SWIR (1850 nm to 2100 nm range, depending on the signal and pump final location). This SWIR light is subsequently amplified in a thulium doped fiber (TDF) of which active ions population inversion is achieved with the remaining L-band pump power at the output of the HNLF, leading to improved power efficiency. In both this former work and the present one a 350 m long HNLF is used. For such a length, we confirmed numerically and

experimentally that dispersion fluctuations due to an uneven core size or a slight birefringence along the fiber lead to a large spectral broadening and a reduction of the theoretically narrow-band parametric gain [8], as can be observed in experiments with short pieces of HNLF or dispersion shifted fibers [9]. In our setup the gain reduction is compensated by the addition of the TDFA whereas the broadening proved to be beneficial for the tuning capacity of the SWIR source. Indeed, the tunability is simply obtained by shifting the signal wavelength and does not require any pump adjustment. In this work, we take further advantage of the broad conversion spectrum of the FOPA to simultaneously convert a fixed O-band signal toward 1950 nm and an additional tunable signal in the 2000-2100 nm band. After this parametric generation process, the 5 waves (2 signals, 2 idlers and 1 pump) at the output of the HNLF are launched into a TDF piece where the idler at 1950 nm undergoes a large amplification thanks to the de-excitation of the  $^3F_4$ - $^3H_6$  transition. In contrast, the idler beyond 2000 nm experiences only a slight gain [10]. In this stage, the L-band pump is mostly absorbed to excite the  $Tm^{3+}$  ions while the two original seeds are strongly attenuated. The remaining waves at the output of the TDF are subsequently launched into a HDF piece where the amplified idler at 1950 nm excites the  $^3I_7$  upper state. The subsequent de-excitation of this latter state then reinforces the longer-wave idler [5] such that the 1950 nm idler becomes the pump for the last holmium stage. A tunable source centered on 2050 nm is finally obtained at the HDF extremity since wavelength selection is achieved by simple tuning of the shorter-wavelength signal at the input of the HNLF. This operating principle is sketched in Fig. 1.

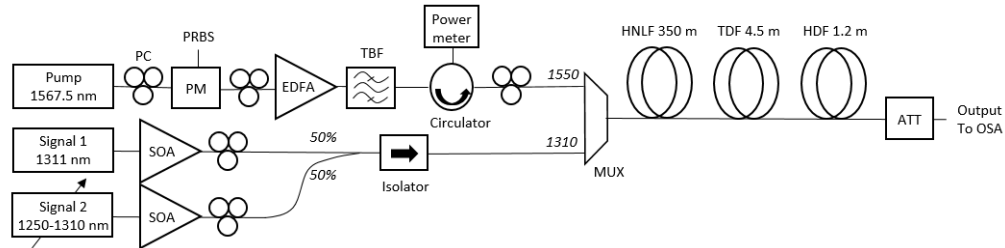


Fig. 2. Experimental setup for SWIR light generation based on parametric conversion and amplification cascade: PC: Polarization controller, PM: Phase modulator, PRBS: Pseudo-random binary sequence, SOA: Semiconductor optical amplifier, EDFA: Erbium-doped fiber amplifier, TBF: Tunable band pass filter, MUX: 1310/1550 nm wavelength multiplexer, HNLF: Highly nonlinear fiber; TDF: Thulium-doped fiber, HDF: Holmium-doped fiber, ATT: optical attenuator.

The detailed experimental setup is described and sketched in Fig. 2. The FOPA section consists of a CW pump from an external cavity laser (ECL) set at 1567.5 nm, phase-modulated with a pseudo-random binary sequence (PRBS) at a bit-rate of 7 GHz to quench stimulated Brillouin scattering (SBS), and amplified through a high power erbium doped fiber amplifier (EDFA). A tunable band pass filter (TBF) is used to remove the amplified spontaneous emission (ASE) and the wave is directed into a circulator used to monitor the power backscattered by SBS. In parallel, one seed (signal 1) is generated by a fixed laser diode emitting at 1311 nm and the other seed (signal 2) by an ECL tunable from 1250 nm to 1310 nm. Each CW signal is then amplified in its own semiconductor optical amplifier (SOA) before being coupled together with a 50/50 coupler followed by an O-band isolator. The signals are then multiplexed with the pump in a 1310/1550 nm wavelength multiplexer and launched into the HNLF. At the input port of the HNLF the power level of the pump is measured to be 34.2 dBm whereas signal 1 is injected at 14 dBm. The launch power of the shorter wave seed (signal 2) varies with wavelength as both the laser power and SOA gain decrease significantly nearing 1250 nm. The HNLF has an average zero-dispersion wavelength (ZDW) of 1569.05 nm, a third-order dispersion coefficient ( $\beta_3$ ) of  $4.6 \cdot 10^{-2} \text{ ps}^3/\text{km}$ , a fourth-order one ( $\beta_4$ ) of  $-2.9 \cdot 10^{-5} \text{ ps}^4/\text{km}$  and a nonlinear coefficient ( $\gamma$ ) of 14

$W^{-1}.km^{-1}$ . After the HNLf, a 4.5 m segment of single mode core-pumped TDF (OFS TmDF200) is directly spliced, followed by a 1.2 m segment of core-pumped holmium-doped double clad fiber (Nufern SM-HDF-10/130) connected through fiber pigtailed. We measured 0.5 dB of loss at 1550 nm at the interface between the HDF and its single-mode fiber pigtailed. A 30 dB C-band optical attenuator was used before the optical spectrum analyzer (OSA). The attenuation function of this element, which strongly depends on wavelength, was experimentally recorded from 1.2 to 2.1  $\mu m$  using a custom build super-continuum source. The measured function was then used to apply numerical correction on the all recorded optical spectra.

### 3. Results and discussions

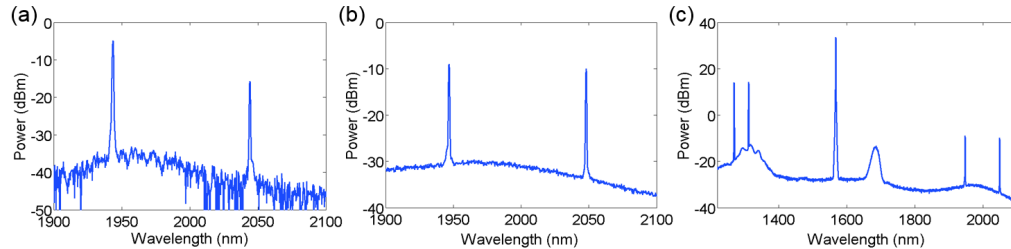


Fig. 3. Spectrum of the SWIR idlers for pumping at (a) 1566 nm and (b) 1567.5 nm. (c) Full-span spectrum of the output of the HNLf pumped at 1567.5 nm. (resolution: 1 nm). Raman scattering peaking at 1685 nm can be observed.

In this triple-stage configuration, tuning of the initial parametric conversion in HNLf is crucial. Indeed, the performance of the subsequent stages will strongly depend on the wavelength and power of the two preliminary SWIR idlers. The conversion efficiency (CE, idler output power over the signal input power) must be simultaneously optimized for two idlers spaced by more than 50 nm. A tradeoff must be met on the L-band pumping wavelength so that each SWIR wave has sufficient amplitude at the output of the HNLf. It is later assessed that on the one hand, both the TDFA and HDFA operate in the linear regime and therefore any power loss on the longer wave idler directly impacts the source's final output power. On the other hand, a poor CE at the short wave idler will diminish the gain in the HDFA stage by reducing its pumping level. This dual-idler adjustment was empirically probed by launching two signals located at 1270 nm and 1311 nm along with a pump, tuned from 1565 nm to 1568 nm. According to measurements recorded after the TDFA and the HDFA an acceptable tradeoff is reached for a 1567.5 nm pump, even though a maximized CE near 1950 nm is obtained for 1566 nm pumping. A comparison of the idlers spectra at the output of the HNLf is presented in Fig. 3. When the pump is set a 1567.5 nm, 5.7 dB are gained on the longer-wave idler while sufficient power is transferred to the shorter wave idler. Additionally, energy conservation in FWM implies that setting the pump further away from the signals will enable the generation of idlers deeper into SWIR.

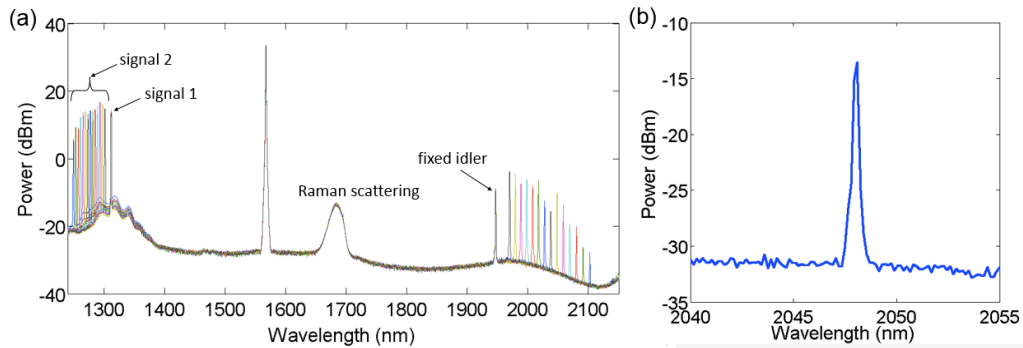


Fig. 4. (a) Superimposed spectra at the output of the FOPA when signal 2 is tuned (resolution: 1 nm). (b) Spectrum of a SWIR idler (resolution: 0.1 nm).

Once the pump wavelength is set, signal 2 is tuned from 1250 nm to 1300 nm, each spectrum is recorded at the output of the HNLF and the results are shown in Fig. 4. The FOPA features an average CE of  $-24$  dB. The maximum idler power of  $-3.9$  dBm is obtained at 1970 nm while at 1947 nm, the wavelength of the idler generated from the fixed signal 1, the CE reaches  $-22$  dB for an output power of  $-8.8$  dBm. It is worth mentioning that due to the low overall CE the FOPA operates in the small signal regime and the idler power could be scaled with the input signal power. While the lack of powerful laser or amplifier in the O-band makes it arduous in practice, several dB could be gained by optimizing the coupling of the two signals. Once the FOPA characterized, the 4.5 m long TDF is spliced to the HNLF. The results at the output of the second stage are summarized in Fig. 5.

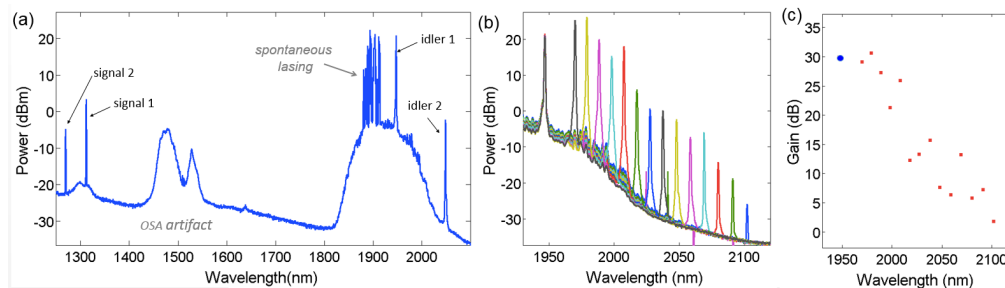


Fig. 5. (a) Spectrum at the output of the TDF when the longer wave idler is generated at 2048 nm. (b) Superimposed spectra of the amplified idlers when the signal is shifted from 1250 to 1300 nm. (resolution: 1 nm). (c) TDF gain for a dual idler input. The gain for the fixed idler is indicated by the blue circle.

The 1947 nm idler, which is the pump for the HDFA, is amplified up to a power of 21 dBm. Due to the relatively low seed power, the 1947 nm wave does not compete for the gain in the TDF: some spontaneous lasing occurs in the spectral region where the emission cross section is the largest, namely around 1880 nm, as seen in Fig. 5(a). This parasitic lasing can easily be suppressed if the 1947 nm seed wave power is increased by a few dB. As already mentioned, a stronger laser at 1311 nm or a lossless multiplexing between the signals would enable the suppression of the 1880 nm lasing. Despite a small fraction of the optical power being lost in the TDF due to this effect, the random laser lines are clearly out of the band of interest and can be easily filtered out. The spectra of the amplified idlers for a tuned signal 2 together with the measured gain of the TDF are shown in Fig. 5(b) and 5(c), respectively. As expected, a maximum gain of 30 dB is obtained near 1950 nm. The longest idler generated (2100 nm) still experiences a couple dB of gain.

Subsequently to this stage and considering the power available at 1947 nm, the HDF length was optimized for broadband amplification of the idlers around 2050 nm, keeping in

mind that the absorption and the emission cross sections of holmium in silica overlap significantly [5]. Following experimental characterization of several fiber lengths, the optimal length was found to be 1.2 m and the spectra obtained at its output are displayed in Fig. 6.

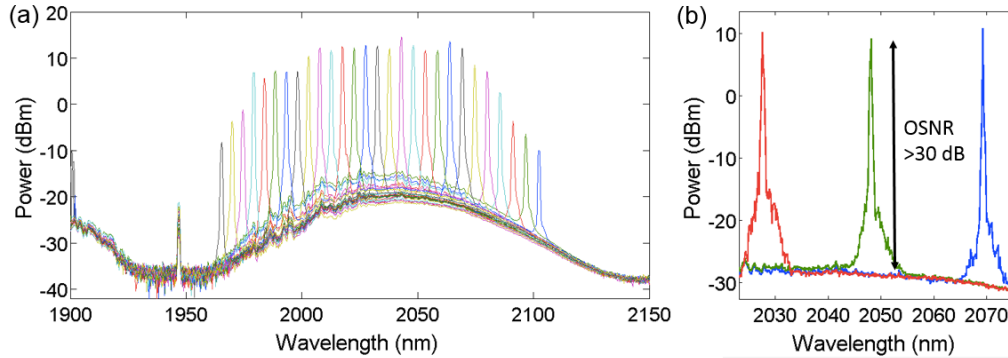


Fig. 6. (a) Superimposed spectra of the amplified idlers when the signal is shifted from 1250 to 1300 nm. (resolution: 1 nm). (b) Spectral zoom on three amplified idlers at 2028 nm, 2048 nm and 2069 nm. (resolution: 0.1 nm).

The 1947 nm pump is strongly absorbed with the holmium absorption cross-section clearly visible, and the energy is transferred to the longer wave idlers. The CW source is capable of delivering up to 15 dBm in the 2010–2070 nm range with a power ripple lower than 3 dB. Overall, the entire 1965 – 2100 nm spectral range is accessible (see Fig. 6(a)). It is worth mentioning that compared to the output of the TDFA, the output power is well equalized beyond 2  $\mu\text{m}$  with the help of the HDF. The L-band pump is totally absorbed and only a slight fraction of the 1947 nm idler flows through the HDF. A higher resolution measurement of three different output wavelengths is shown in Fig. 6(b). Considering that all the out-of-band noise could be filtered out after the setup with a suitable device, an OSNR of at least 30 dB is maintained over the 2010 – 2070 nm range.

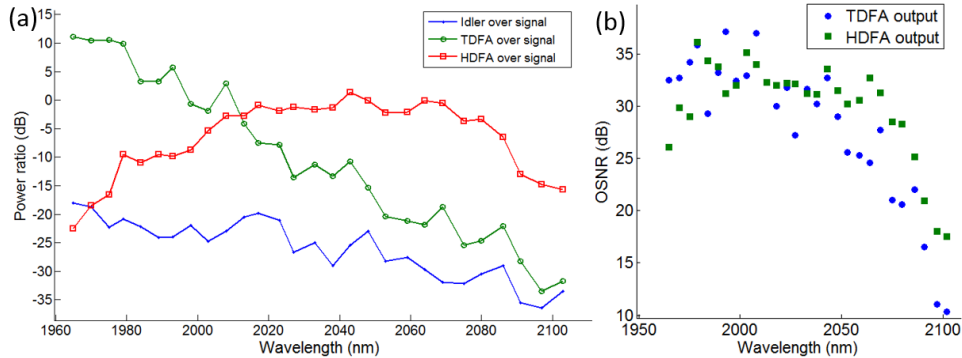


Fig. 7. (a) Ratio of the idler power over its corresponding signal power, as measured before the HNLF, after the conversion in the FOPA (blue), the amplification in the TDFA (green) and the amplification in the HDFA (red). (b) Optical signal to noise ratio for the tunable idler after TDF (blue) and HDF (green). These ratios were computed for a set of wavelength between 1970 and 2100 nm.

To underline the benefit of adding a HDF segment, the ratio of the SWIR waves power over their corresponding seed power as measured at the input of the HNLF, was computed for the whole range of wavelength after each of the three stages (FOPA, TDFA and HDFA). The result is displayed in Fig. 7(a). A clear red-shift of the conversion efficiency is observed after the HDFA. The conversion efficiency is above transparency for idlers located between 2010 – 2080 nm which is a significantly improvement (25 dB on average) compared to standard

HNLF parametric conversion. In terms of overall power efficiency in the amplifier (HNLF-TDF-HDF) from the pump toward the tunable idler, neglecting the signal power as it 100 times lower than the pump's, a figure of  $-20$  dB is reached at 2043 nm. Figure 7(b) also demonstrates that the output OSNR is improved at longer wavelengths thanks to the addition of the HDF.

#### **4. Conclusion**

A SWIR laser source delivering up to 20 mW, of which the wavelength can be freely selected from 2  $\mu\text{m}$  to 2.1  $\mu\text{m}$  is reported. This source is based on an original design that embeds a silica-fiber based parametric wavelength converter, operating over more than 750 nm, assisted by SWIR gain obtained successively in a TDF and a HDF. Dispersion fluctuations in the HNLF are leveraged to obtain a broadband conversion that allows for the simultaneous generation of the HDFA pump seed and of the SWIR output. The three amplification stages are pumped successively using the same L-band laser and apart from the fibers, all elements used in this experiment are off-the-shelf devices intended originally for telecommunication purposes. Additionally, multi-GHz intensity modulation of this source is possible by modulating the shorter-wave O-band signal with a standard communication modulator at the input of the parametric amplifier, as shown by previous works [11, 12]. Further ongoing work concerns the reduction of the output phase noise, and consequently of its linewidth, with the help of a dispersion-stabilized and stress-insensitive HNLFs to quench SBS in place of pump phase dithering.

#### **Acknowledgment**

This work is supported by the European Research Council under grant agreement ERC-2012-StG 306630-MATISSE. The authors would like to thank Sumitomo Electric Industries for providing the HNLF.